Frontiers in Health Informatics
ISSN-Online: 2676-7104
www.healthinformaticsjournal.com
2024; Vol 13: Issue 3
Open Access

Formulation, optimization and characterization of Mfx-Gold nanoparticle loaded in-situ gel for ophthalmic drug delivery using box-benken design approach

Nagendra Bhuwane[1], Preeti K. Suresh[1]*
[1]University Institute of Pharmacy, Pt. Ravishankar Shukla University, Raipur (C.G.)
suresh.preeti@gmail.com

Cite this paper as: Nagendra Bhuwane, Preeti K. Suresh (2024) Formulation, optimization and characterization of Mfx-Gold nanoparticle loaded in-situ gel for ophthalmic drug delivery using box-benken design approach. *Frontiers in Health Informatics, 13* (3), 779-805.

Abstract
The aim of the present investigation is to prepare and evaluate Mfx-GNPs loaded in-situ gel-for ophthalmic drug delivery system. The study is proposed to evaluate the anti-bacterial and anti-biofilm efficacies of Mfx-GNPs loaded in-situ gel. This article describes a systematic approach for the design, optimization, and characterization of Mfx-GNPs loaded in-situ gel. Optimization was performed using a 3^2 response surface approach, the effect of Concentration of Gellan gum (X_1), Concentration of Chitosan (X_2) and Concentration of Carbopol 940p (X_3) content was optimized as independent variables, Viscosity at non physiological condition (Y_1) and Viscosity at physiological condition (Y_2) served as variables. The optimized formulation is characterized by EE, particle size, Fourier transform infrared spectroscopy (FTIR), Xray diffraction (XRD), differential scanning calorimetry (DSC), scanning electron microscopy (SEM), in vitro drug release study, antibacterial efficacy and antibiofilm activity. The percentage of EE is 89%, the size is 56.25 nm, and the in vitro drug release is 92%. Mfx-GNPs loaded in-situ gel are fully prepared and can effectively release drugs in a sustained mode.

KEY WORDS: *Gold Nanoparticles (GNPs), Moxifloxacin (Mfx), Anti-biofilm, In-Situ Gel.*

INTRODUCTION:

Delivering and maintaining the ideal drugs concentration at the site of action within the eye is one of the main challenges in ocular delivery. A range of ophthalmic dose forms, including gels, ointments, solutions, and polymeric inserts, have been studied in an effort to prolong the duration of pharmaceutical ocular occupancy for topical application to the eye. Makwana et al., 2016.These dose forms have improved the corneal contact time to varied degrees. However, due to issues like ointments causing blurred vision or inserts causing patient noncompliance, they have not been widely used. Baranowski et al., 2014. Because the eye drops rapidly wash out during eye lachrymation, their bioavailability is relatively low. The majority of the systems are used as solutions or suspensions. With traditional ocular formulations, there is a rapid pre-corneal clearance that results in low drug bioavailability. When a highly viscous solution or gel is easy to administer, patient compliance and its use are delayed. The in-situ gel dosage form is associated to both lachrymation and blurred vision. Akhter et al., 2022. Therefore, they could be avoided by developing a drug formulation that, when administered topically, forms an instantaneous in situ gel. After instillation, they undergo gelation because of physico-chemical changes take place in the eye. Formulating an in situ gel improves the drug's bioavailability and extends its pre-corneal residence time. Vigani et al., 2020. A significant issue in ocular therapies is achieving the ideal drug

concentration at the site of action, which is hampered mostly by pre-corneal loss, which leaves the eye with just a small amount of the drugs absorbed. By using in situ gel-forming techniques to extend the duration of drug retention in the eye. Mandal et al., 2012

A lot of bacteria have the potential of assembling into a three-dimensional, strong network known as a "biofilm." Biofilm provide the adhesion, nutrition, and protection to bacterial cell. Pathogenesis, disease progression, and resistance to nearly all traditional antibiotics are all affected by them. The use of gold nanoparticle against bacterial biofilms has the need for novel antimicrobial drugs. Zhao et al., 2023. Through a variety of ways, these nanoparticles and their associated ions cause damage to the components and structure of biofilms as well as disrupt bacterial metabolism. These nanoparticles approach the biofilm, penetrate it, travel inside, and interact via electrostatic, hydrophobic, hydrogen-bonding, Van der Waals, and ionic interactions with essential biofilm constituents like polysaccharides, proteins, nucleic acids, and lipids in order to exert their antimicrobial activity. Joshi et al., 2020. Through comparable interactions, a small number of bacterial biofilms also exhibit resistance to these nanoparticles. Shkodenko et al., 2020. The physicochemical characteristics of biofilm and nanoparticles determine the nature of these interactions and the overall antibacterial impact. Therefore, it is crucial to investigate these interactions and the molecule players involved in order to manipulate the characteristics of nanoparticles and achieve the best possible antibacterial effects against a variety of bacterial infections. Wang et al., 2017.

The physicochemical properties of GNPs, including their tunable core size, photothermal and photodynamic properties, high chemical stability, biocompatibility, high X-ray absorption coefficient, efficiency in producing ROS, and localized surface plasmon resonance (LSPR) properties, are responsible for their wide range of applications. Tarantino et al., 2023; Gu et al.,2021 GNPs shows instance, damage of bacterial cell membranes and reduce their rate of metabolism. The small size of the nanoparticles makes gold colloid potentially prone to nanoparticles aggregation. Yang et al., 2007. In order to stabilize GNPs, additives like polyelectrolytes or polymers are typically used. By acting as capping or protective agents, these stabilizers stop aggregation brought on by steric hindrance. Rabiee et al., 2022.

Some important characteristics of GNPs, such as size and shape have been tailored and explored to improve the antibacterial activity of the in-situ gel. Su et al., 2020. The latest advances in gold nanoparticles embedded in in-situ gel for the treatment of multidrug-resistant bacterial infections. Zhao et al., 2022. The efficiency of GNPs against pathogenic bacteria is presented from three relevant aspects: antibacterial activity, anti-biofilm activity. Das et al., 2021.

MATERIAL AND METHODS

Materials:

Pure drug moxifloxacin Hydrochloride was received as a gift sample from Anant Pharmaceuticals Pvt. Ltd., Maharashtra, India. Chloroauric acid, tri-sodium citrate, gellan gum and chitosan were procured from Molychem,Mumbai, India. The nutrient agar media and bacterial strains was purchased from Hi-Media, India. All the otherreagents were used in the present study were of analytical grade.

Determination of λ max of moxifloxacin hydrochloride

For the preparation of calibration curve 100 mg of the drug was weighed, dissolved in 100 ml of volumetric flask, and the volume was adjusted with STF to prepare the stock solution (1000 mg/ml) which is used to determine the absorption maxima. A 100 ml of volumetric flask was filled with 10 ml of standard stock solution,

and volume was adjusted with STF to produce 100 mg/ml of moxifloxacin. The stock solution was divided into 0.2, 0.4, 0.6, 0.8, and 1.0 ml volumetric flasks, and the volume was made up with STF to the appropriate mark. This process was used to prepare serial dilutions with concentrations of 2, 4, 6, 8, and 10 mg/ml. UV-visible spectrophotometer UV 1900, Shimadzu, was used to scan the resultant solution between 200 and 400 nm. Koirala et al.,2021.

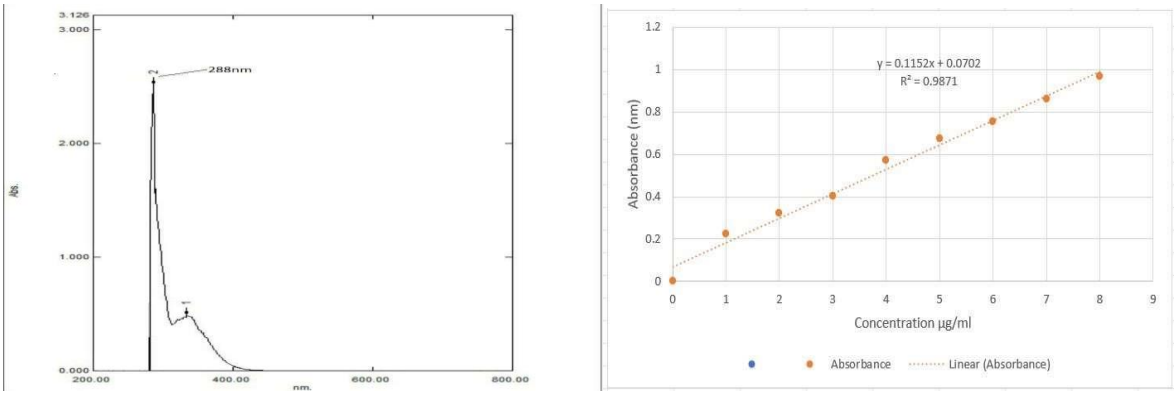

(A) **(B)**

Figure 1: (A) UV Spectra of Moxifloxacin Hydrochloride (B) Calibration Curve of Moxifloxacin Hydrochloride at (λ max) 288 nm in STF

Method of Preparation:

Synthesis of Mfx-Gold Nanoparticle

For the synthesis of Mfx-GNPs, trisodium citrate was used as a moderate reductant throughout the synthesis of Mfx-GNPs. Deionized water was used to prepare solutions of the ligand (1 mM moxifloxacin) and metal salts (1 mM HAuCl4). Different quantities of solutions containing noble metal salts and moxifloxacin were mixed to perform the reactions. Then after vigorously stirring the reaction mixture at room temperature for approximately half an hour, 0.2 ml of 50 mM trisodium citrate were added dropwise. The formation of the required Mfx-GNPs was indicated by a gradual change in the color of the solution. The addition of the reducing agent convert the bright yellow solution to maroon, then brown, and finally ruby red, depending on the metal to ligand molar ratio. Dong et al.,2020; Nisar et al.,2015.

Formulation of Mfx-GNPs Loaded In-Situ Gel

Preparing a medicated formulation for bacterial infections of the eyes: moxifloxacin eye drops are typically sold as a 0.5% w/v drug solution. Because of this, the formulation was prepared with a dosage of 0.5%. Gellan gum, chitosan, and carbopol 940p were chosen as the polymers and co-polymers, respectively. The cold method was used to prepare a polymer solution. In summary, the precise amount of gellan gum or chitosan, either alone or combined with carbopol 940p, was determined. The required volume of distilled water was then added, together with the estimated quantity of Mfx-GNPs, and the mixture was continuously stirred for 15 minutes (Remi Instruments, India). 0.1% methyl paraben was added as a preservative. To make the solution isotonic, the required quantity of glycerol was added and carefully mixed. The mixture was transferred into amber-colored bottles. The final solutions were autoclaved for 20 minutes at 15 psi and 121°C to sterilize them. Zafar et al.,2022; Nair et al.,2021.Mfx-GNPs loaded in-situ gel is shown in table.

Table 1: Formulation Table of Mfx-GNPs Loaded In-Situ Gel

S. No.	Ingredients	Concentration (W/V)
1.	Mfx-GNPs	0.5%
2.	Chitosan	0.75%
3.	Gellan Gum	0.625
4	Carbopol 940p	0.375%
5	Glycerol	q.s.
6.	Methyl Paraben	0.1%
7.	Purified Water q.s.	100%

Experimental Design:

Box-Behnken experimental design

The Box-Behnken Design (BBD) was used to statistically optimize the formulation parameters and to evaluate the main effects, interaction effects and quadratic effects of the formulation ingredients on the performance of the in-situ ocular gelling systems Zhu et al.,2009; Yadav et al.,2020.This three factor, two level design was used to explore the quadratic response and to construct the second order polynomial models using Design Expert Software. The Box-Behnken design was selected, as it requires few runs than other two level response surface design models. This cubic design is characterised by the set of points lying at the midpoint of each edge in a multidimensional cube and the center point replicates (n = 5), whereas the 'missing corners' help the experimenter to avoid the combined factor extremes. Kalbhare et al.,2021 A design matrix comprising of 17 experimental runs was constructed as shown in table 2. The non-linear computer generated quadratic model is given as:

$$Y_1 = B_0 + AX_1 + BX_2 + CX_3 + ABX_1X_2 + AC\,X_1X_3 + BC\,X_2X_3 + A^2X_1^2 + B^2X_2^2 + C^2X_3^2$$

Where, Y_1 is the measured response associated with each factor level combination; B_0 is an intercept; A to C^2 are estimated regression coefficients computed from the observed experimental values of Y_1; and X_1, X_2 and X_3 are the coded levels of the independent variables. The terms X_1X_2 and X^2 i (i = 1, 2 or 3) represent the interaction and quadratic terms, respectively. The main effects (X_1, X_2 and X_3) represents the average results of changing one factor at a time from its low to high value. The interaction term (X_1X_2) shows how the response changes when two or more factors are simultaneously changed. The dependent and independent variables selected for the Mfx-GNPs loaded in situ gelling systems are shown in Table:3 along with their low (-1), medium (0) and high (+1) levels, which were selected based on the results of the preliminary experiments. The table: 3 also shows the constraints for various responses/dependent variables (Y_i) which need to be optimized to formulate an ideal in-situ gelling system for ocular application.

Table 2: Box Behnken Design matrix with transformed values

Batches	X_1	X_2	X_3
1	0	0	0
2	1	0	-1
3	-1	0	1
4	0	-1	1
5	-1	1	0

6	0	1	-1
7	0	0	0
8	0	-1	-1
9	0	0	0
10	1	-1	0
11	-1	-1	0
12	-1	0	-1
13	0	0	0
14	0	0	0
15	0	1	1
16	1	1	0
17	1	0	1

Table 3: Independent and dependent variables for ocular in-situ gelling systems

Independent Variables	**Levels**		
	Low	**Medium**	**High**
X_1: Concentration of Gellan gum (%W/V)	0.5	0.6	0.75
X_2 : Concentration of Chitosan (%W/V)	0.5	0.6	1
X_3 : Concentration of Carbopol 940p (%W/V)	0.30	0.35	0.45
Dependent Variables	**Constraints:**		
Y_1 : Viscosity (cps) at non physiological condition (25^0C, pH 5)	**Y_1**		Minimum
Y_2 : Viscosity (cps) at physiological condition(35^0C, pH 7.4, STF)	**Y_2**		Maximum

Characterization of optimized formulation

Entrapment Efficiency

Using spectrophotometric analysis (UV 1900, Shimadzu, Japan), the total percentage of drug entrapped (% EE) was determined. Centrifuging the sample at 12000 rpm and 5ºC for 30 minutes (Cooling Centrifuge, Remi Instruments Ltd., Mumbai, India) separated the unentrapped drug in the dispersion (Das et al., 2010). The supernatant was decanted and the concentration of Mfx-GNPs loaded in-situ gel was measured spectrophotometrically at 288 nm. The experiment were carried out in triplicate. % EE has been calculated by using following formula Lv et al.,2018.

$$\% \text{ EE} \quad \frac{\textbf{Total drug used – Unentrapped drug}}{\textbf{Amount of drug used in preparation}} \quad \textbf{X 100}$$

Mean particle size, polydispersity index (PDI) and zeta potential

Photon correlation spectroscopy (PCS) (Zetasizer Nano ZS 90, Malvern Instruments, UK) was used to evaluate the prepared Mfx-GNPs for mean particle size, size distribution, zeta potential, and PDI. In order to measure the particle size, the prepared Mfx-GNPs colloidal solution was diluted with Millipore ultra-pure distilled water, filtered through whatman filter paper (0.22µm), and then the particle size was measured at 25^0C and 90^0 fixed angle. Zeta potential is a crucial physicochemical factor that affects the stability of a colloidal nanosystem. Maximum repulsion between identical charged particles avoids aggregation and confirms redispersibility, however extreme positive or negative values provide a strong repulsive force. Hussain et al.,2020; Karimi et al.,2019.

Scanning Electron Microscopy (SEM)

To confirm the Mfx-GNP production and analyze the morphology of the produced Mfx-GNPs, scanning electron microscopy (SEM) was used. A JSM-6610LVnx (Jeol, Tokyo, Japan) device with an integrated energy dispersive X-ray spectroscopy (EDS) system from Aztec Energy (UK) and a high-resolution CCD camera was used to take the SEM pictures. The Mfx-GNPs solution was dropped into a copper holder that had been covered with chromium film, and let to dry. SEM pictures were taken at magnifications ranging from 15,000× to 18,000×. A 20–25 kV accelerating voltage was employed. Dzimitrowicz et al., 2019.

Fourier Transforms Infrared Spectroscopy (FTIR)

FTIR (Fourier Transformer Infrared Spectroscopy) was employed with 0.1 mm KBR pellets to determine the drug excipient compatibility analysis. To assess the interaction, the infrared spectra of the drug in its pure form, (moxifloxacin Hcl), and all of the excipients are compared. Chadha and Bhandari. 2014.

Differential Scanning Calorimetry (DSC)

DSC thermograms of the pure drug Mfx and the physical mixture of gellan gum, chitosan, and carbopol 940p were obtained using a thermal DSC analyzer (Shimadzu, Singapore DSC − 60). The sample was weighed precisely in an aluminum pan, crimped with an aluminum cover, and heated from 20.0 °C to 300.0 °C at a rate of 20 °C per minute. Kalaria et al., 2023.

X-Ray Diffraction (XRD) Analysis

To determine whether the Mfx was crystalline or amorphous, X-ray diffraction (XRD) was used. Using an X-ray diffractometer (PANalytical equipped with an XPERT-PRO Diffractometer System, Germany) operating at 35kW and 20 mA across a 2Θ range of 5 to 70°, the sample was analyzed for X-ray diffraction patterns. A scanning rate of 1° min^{-1} (20 Θ) was used. Endla and Radhika.2021.

Clarity

The visual clarity of gelling solutions was assessed in light on a white and black background. Srividya et al., 2001.

Gelling capacity

A drop of the resulting formulation was added to a vial containing 2ml of the freshly prepared simulated tear

fluid. The composition of the simulated tear fluid (STF) was: NaCl 0.67 g, $NaHCO_3$ 0.2 g, $CaCl_2.2H_2O$ 0.008 g and water up to 100 ml, Nayak et al., 2012. And the gelling capacity of the mixture was then measured visually. The duration required for its gelling was observed. Liu et al., 2010; Narayana et al., 2022.

Rheological studies

The Brookfield viscometer model LVDV-E was used to test viscosity. The sampling tube was filled with the in situ gel formulation. Before every measurement, the samples were examined in a circulating bath that was attached to the viscometer adapter which maintained at 37°C ± 0.5°C. The viscosity of the formulation was determined after increasing the spindle's angular velocity by 1 to 4. Mandal et al.,2012.

Measurement of pH

The pH of the developed in-situ gel compositions was measured with a digital pH meter that was calibrated. Before each usage, the pH meter was calibrated using standard buffer solutions with pH values of 4, 7, and 9. The formulations were kept at 25 ℃ in temperature. An electrode was placed on the formulation's surface to monitor pH. Garala et al.,2013.

Sterility Studies

In compliance with Indian Pharmacopoeia (I.P.) guidelines, a sterility studies was carried out to determine the bacterial growth of Mfx-GNPs loaded in-situ gel using the direct inoculation method. Initially, two digest media were used: soyabean casein digest medium and fluid-thioglycollate medium. Then, two test tubes containing 10 mL of fluid-thioglycollate medium and 10 mL of soyabean-casein digest media each were aseptically filled with 2 mL of the developed formulation using a sterile pipette. These were incorporated with the media and then incubated for a minimum of 14 days at 30–35°C for fluid-thioglycollate medium and 20–25°C for soyabean-casein digest medium. A blank containing only digest media and a positive control with a mixture of digest media and any kind of microorganism were also included. After 14 days, a comparison was done between the test, blank, and positive control samples in order to determine the rate of bacterial growth Andhale et al., 2023.

Drug content

To determine the drug content of the prepared Mfx-GNPs loaded In-Situ gel, 50 mg of drugs from each formulation were dissolved in 50 ml of water. After an appropriate dilution, the drug content was determined spectrophotometrically at 288 nm. The experiment was performed in triplicate. Sriamornsak et al.,2010.

In vitro Drug Release Study

The Mfx-GNPs loaded In-Situ gel was subjected to in vitro drug release studies utilizing a modified Franz's diffusion devices equipped with a dialysis membrane (MW cut off 10,000Da). Simulated tear fluid (STF) (pH 7.4) was used to pretreat the dialysis membrane for 24 hours at 37^0C while being stirred in a water bath. The 2ml aqueous dispersion of the developed formulation was added to the donor chamber while the receptor cell continuously stirred at 100 rpm and maintained STF (pH 7.4) at 37 ± 0.5^0C. To maintain the sink conditions, 2 ml of the sample was taken out of the receptor compartment and replaced with 2 ml of fresh STF at regular intervals (0, 1, 2, 3, 4, 5, 6, 8, 10, 12, and 24 hours). For Mfx-GNPs loaded In-Situ gel, the amount of drug released in the receptor compartment was measured using UV spectrophotometry (Shimadzu UV-1900, Japan) at 288 nm Kalaria et al., 2023. A graph showing the percentage drug release over time was plotted after the percentage drug release was determined. For every formulation, the release experiments were carried out in triplicate.

Antimicrobial activity

The antibacterial activity of Mfx-GNPs loaded in-situ gel was investigated using the standard well diffusion method against Pseudomonas aeruginosa (ATCC27853) Escherichia coli (ATCC25922), Staphylococcus aureus (ATCC25923), Candida albicans (ATCC14053) and Klebsiella pneumoniae (ATCC700603). Freshly formed culture was spread on sterilized nutrient agar plates, and 8 mm wells in the agar plates were made with a sterile cork borer. The wells were loaded with 2µg/ml concentrations of Mfx-GNPs loaded in-situ gel and 2µg/ml of Mfx was serving as a control. After that, the plates were maintained at 37 °C for a day, and the antibacterial activity of the Mfx-GNPs loaded in-situ gel was determined by measuring zones of inhibition (ZOI) around the well impregnated with Mfx-GNPs loaded in-situ gel. Bao et al., 2013.

Anti-Biofilm Activity

Anti-biofilm activity is measured by evaluating the role of gold nanoparticles at various concentrations upon already established mature Staphylococcus aureus (ATCC25923) biofilm on a glass coverslip. Further, the coverslips were stained with crystal violet (CV) dye followed by imaging under microscope. Berini et al., 2021.

Accelerated stability study

A 45-days short-term accelerated stability study was conducted on the formulations. The samples were kept in a refrigerator (2 to 80 ^{0}C), at ambient temperature, and at elevated temperatures (such as 40 ^{0}C at 75% RH). Samples were taken out at weak intervals and examined for drug content, pH, gelling capacity, clarity, and appearance. Mandal et al., 2012.

RESULT AND DISCUSSION:

Box-Behnken Design

Data Analysis in Box-Behnken Design

All the responses (dependent variables) observed for the 17 batches were simultaneously fitted to the quadratic response surface model using design expert software. The observed responses/dependent variables (Y_1, Y_2) for the Mfx-GNPs Loaded in-situ gelling system are shown in Table 4.

Table 4: Measured response (Y_1, Y_2) of Box Behnken Design

Batch No	Concentration of Gellan gum (%W/V) (X_1)	Concentration of Chitosan (%W/V) (X_2)	Concentration of Carbopol 940p (%W/V) (X_3)	Viscosity (cps) non physiological condition (Y_1)	Viscosity (cps) physiological condition (Y_2)
1	0.625	0.75	0.375	630.25 ± 0.02	470.14 ± 0.02
2	0.625	1	0.3	6675.45 ± 0.16	6879.25 ± 0.01
3	0.5	0.5	0.375	3330.12 ± 0.09	3540.64 ± 0.02
4	0.5	0.75	0.45	1065.41 ± 0.04	1400.15 ±0.03
5	0.625	0.5	0.45	4545.35 ± 0.12	4600.12 ± 0.01
6	0.75	1	0.375	5295.32 ± 0.74	5239.24 ± 0.01
7	0.625	0.5	0.3	5280.45 ± 0.19	5620.16 ± 0.02
8	0.625	0.75	0.375	3870.45 ± 0.19	3200.12 ± 0.02
9	0.625	0.75	0.375	4230.23 ± 0.21	1548.24 ± 0.01
10	0.625	1	0.45	9780.12 ± 0.11	9100.14 ± 0.04

11	0.5	0.75	0.3	5865.78 ± 0.11	5910.65 ± 0.01
12	0.75	0.5	0.375	1023.35 ± 0.12	1138.65 ± 0.02
13	0.75	0.75	0.3	1935.54 ± 0.15	1500.15 ± 0.03
14	0.5	1	0.375	1860.75 ± 0.15	1578.27 ± 0.02
15	0.625	0.75	0.375	2687.62 ± 0.15	2440.67 ± 0.01
16	0.625	0.75	0.375	3946.52 ± 0.05	3708.16 ± 0.03
17	0.75	0.75	0.45	4853.74 ± 0.14	4841.66 ± 0.03

Data analysis for Y_1 (Viscosity at non-physiological condition)

The measured viscosity values (630 to 9780 cps, Table 3) at the non-physiological condition were lower in comparison to the physiological condition. The high variation in the values clearly indicates that the viscosity at non-physiological condition (Y_1) was strongly affected by the selected independent variables. The response (Y_1) obtained at various levels of the three independent variables were subjected to the multiple regression analysis to give a quadratic polynomial equation (1).

$$Y1=3072.60X_1+123.25X_2+1179+6X_3+1435.50X_1X_2+1929.50X_1X_3+960X_2X_3-1668.05X_1^2+ 1472.45\ X_2^2+2024.95\ X_3^2 \ldots\ldots.(1)$$

The non-linear model generated for viscosity at the non-physiological condition was found to be significant with an F-value of 4.44, P value < 0.05 and R^2 value of 0.8544. Out of the three independent variables, the X_1 = 0.625 (Gellan gum) and X_2 = 0.75 (Chitosan) and X_3 = 0.375 (Carbopol) showed prominent positive effect on the viscosity at the non-physiological conditions (Table 4)

Data analysis for Y_2 (Viscosity at physiological condition)

The observed viscosity values at the physiological condition varied from 470.1 to 9100.1 cps. The results clearly indicate that the viscosity at the physiological condition (Y_2) was strongly affected by the selected independent variables under study. The non-linear model was found to be significant with an F-value of 4.56, P value < 0.0289 and R2 value of 0.8544. The response (Y_2) obtained at the various levels of the three independent variables were subjected to multiple regression to give a quadratic polynomial equation (2).

$$Y_2 = 2873.42+36.25\ X_1+987.16\ X_2+3.99\ X_3 +1515.75\ X_1\ X_2+1963\ X_1\ X_3 +810.23\ X_2\ X_3 -1568.02\ X_1^2+1568.75\ X_2^2+2107.70\ X_3^2 \ldots\ldots\ldots(2)$$

At the physiological condition, the viscosity of the in situ gel was significantly increased and was strongly affected by X_1 = 0.625 (Gellan gum) and X_2 = 0.75 (Chitosan). And X_3 = 0.375 (Carbopol 934P) did not affect the viscosity significantly (Table 4).

Table 5: Analysis of variance (ANOVA) for all responses

Source	**Y_1 : Viscosity at non physiological condition**			**Y_2 : Viscosity at physiological condition**		
	Coded coefficient	**F Value**	**p value**	**Coded coefficient**	**F Value**	**p value**
Model	3072.60	4.44	0.0310 **(Significant)**	2873.42	4.56	0.0289 **(Significant)**
X_1	123.25	0.0647	0.8065	36.25	0.0059	0.9411

X_2	1179	5.92	0.0452	987.16	4.35	0.0753
X_3	61	0.0159	0.9034	3.99	0.0001	0.9935
$X_1 X_2$	1435.50	4.39	0.0744	1515.75	5.13	0.0579
$X_1 X_3$	1929.50	7.93	0.0259	1963	8.61	0.0219
$X_2 X_3$	960	1.96	0.2039	810.23	1.47	0.2652
X_1^2	-1668.05	6.24	0.0411	-1568.02	5.78	0.0471
X_2^2	1472.45	4.86	0.0633	1568.75	5.79	0.0471
X_3^2	2024.95	9.19	0.0191	2107.70	10.45	0.0144
R^2	0.8510 **(Quadratic)**	-	-	0.8544 **(Quadratic)**	-	-

Contour plots and response surface analysis

The effect of independent variables on the response was further elucidated using the contour plots (Fig.2). It was determined from the contour plot (Fig. 2, A) that, the target viscosity (easily pourable) of 630 to 9780 cps at the non-physiological condition could be achieved with the X_1 level (concentration of gellan gum, %w/v) ranging from 0.25 to 0.75 %w/v ,the X_2 level (concentration of Chitosan, %w/v) ranging from 0.25 to 1 %w/v and the X_3 level (concentration of Carbopol 940p, %w/v) ranging from 0.15 to 0.45 %w/v The contour plot (Fig. 2, B) shows the effect of X1 and X2 and X_3 on viscosity at the physiological condition (Y_2). The viscosity increased with increase in the concentration of the polymers. However, the target viscosity (470.1 to 9100.1 cps) can only be achieved at combination of (X1 = 0.25 to 0.75 %w/v and X2 = 0.25 to 1 %w/v and X_3 = 0.15 to 0.45 %w/v).

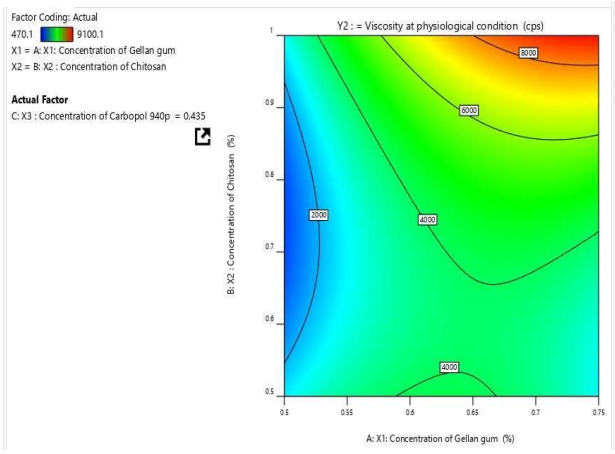

(A)

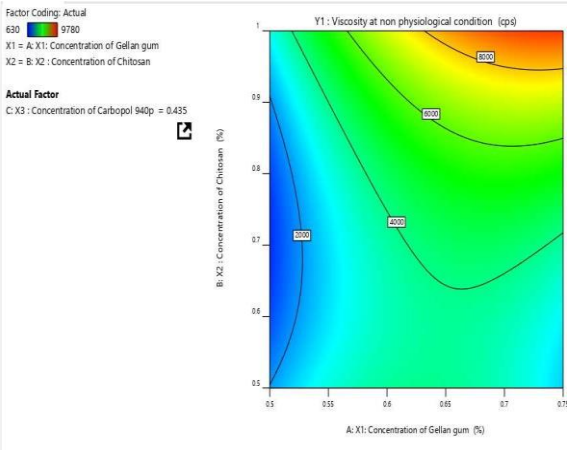

(B)

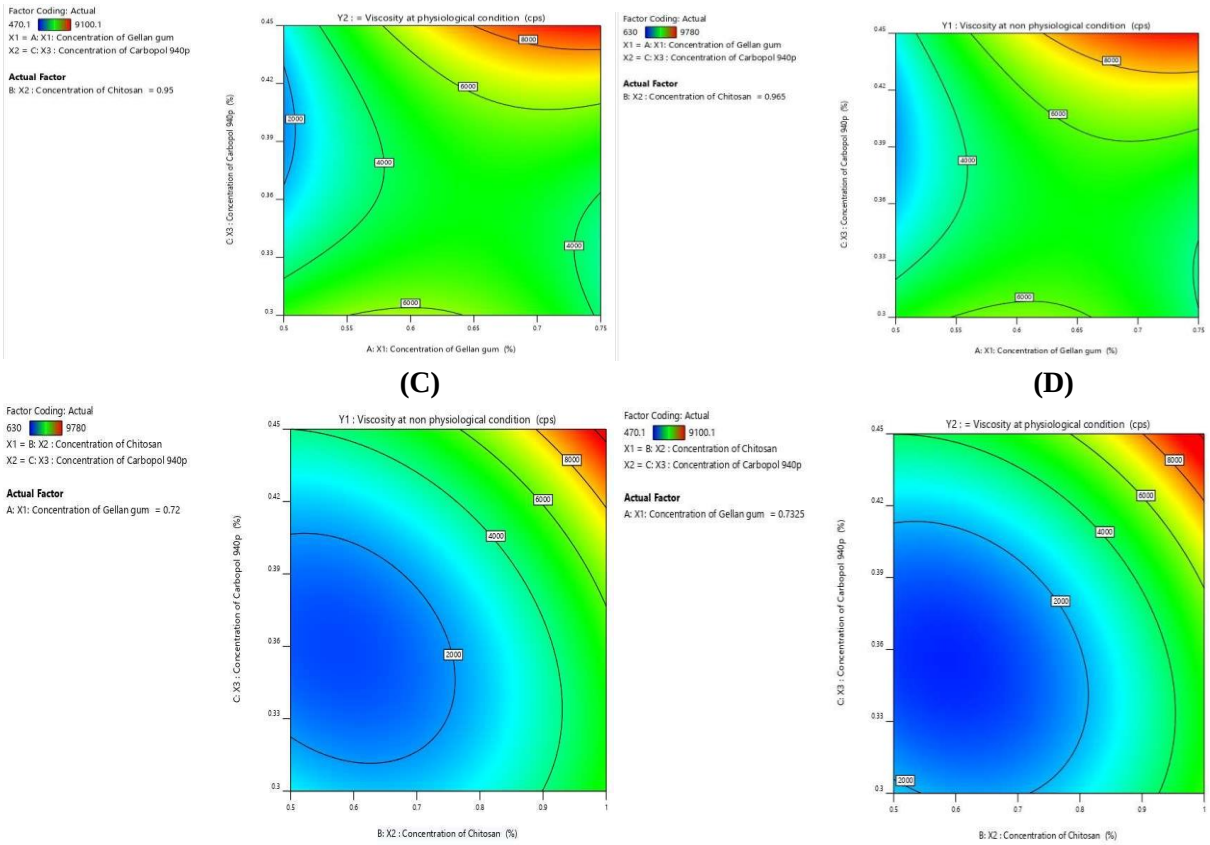

Figure 2: Contour plots showing the effect of studied independent variables **(A)** X1 and X2 on viscosity at non-physiological condition (Y_1) **(B)** X1 and X2 on viscosity at the physiological condition (Y_2) **(C)** X1 and X3 on viscosity at non physiological condition (Y_1) **(D)** X1 and X3 on viscosity at the physiological condition (Y_2) **(E)** X2 and X3 on viscosity at non- physiological condition (Y_1) **(F)** X2 and X3 on viscosity at the physiological condition (Y_2).

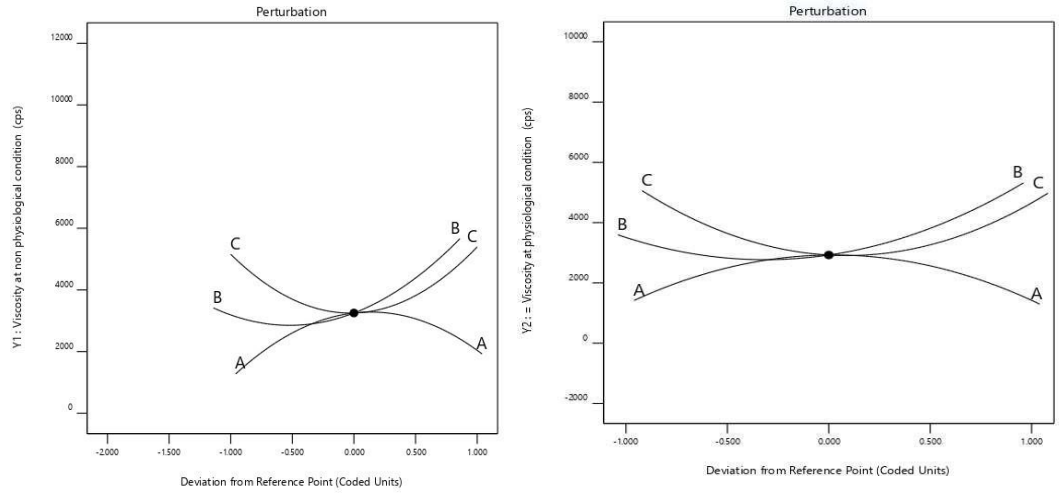

Figure 3: Perturbation graph showing the effect of studied independent variables(X_1, X_2, and X_3) on **(A)** Viscosity at

non-physiological condition (Y_1) **(B)** Viscosity at the physiological condition (Y_2).

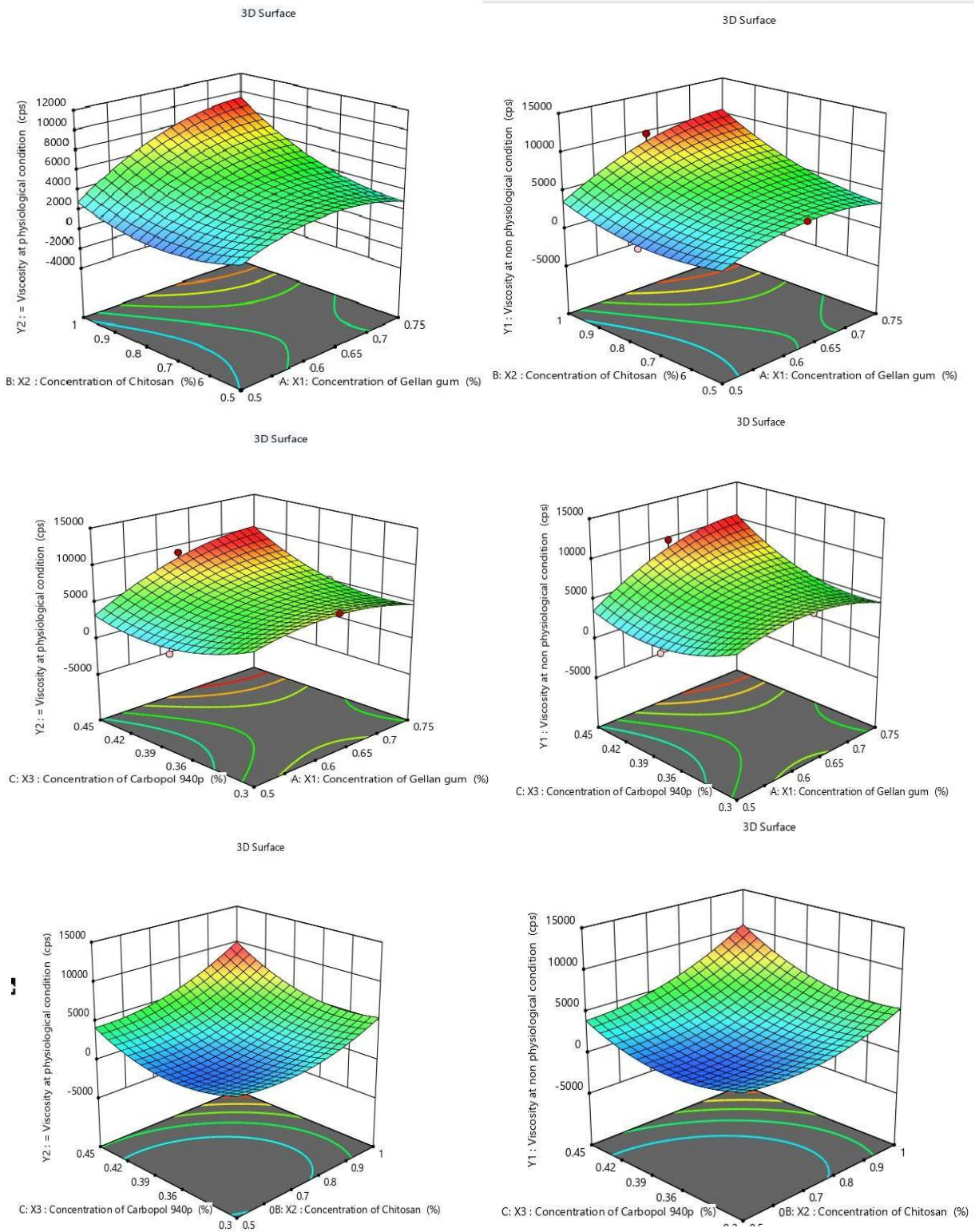

Figure 4: Response surface plots showing the effect of studied independent variables(X_1, X_2, and X_3) on viscosity at

non-physiological condition (Y_1) and viscosity at the physiological condition (Y_2).

Optimization

Based on the statistical studies of the effect of the independent variables [X_1 = Concentration of Gellan gum (% w/v), X_2 = Concentration of chitosan (% w/v) and X_3 = Concentration of Carbopol 940p (%w/v)] on the responses, the level of the independent variables which contribute the optimum response (Y_1= 630 to 9780 cps, Y_2= 470.1 to 9100.1 cps) were determined. Keeping all the constraints in view, from the contour plot the level of X_1, X_2 and X_3 were selected using the Design Expert Software. The software recommended the optimum batch with 0.99 desirability, by selecting (grid search) X_1 = 0.625%w/v, X_2 = 0.75%w/v and X_3 = 0.375%w/v, to get the model predicted viscosity = 3072.6 cps at the non-physiological condition, viscosity = 2873.42 cps at the physiological condition.

Table 6: Regression analysis results for Y_1 and Y_2

Response	R^2	Adjusted R^2	Predicted R^2	SD	CV%	Adeq. Precision
Y_1	0.8510	0.6594	0.0647	1370.43	84.84	7.9769
Y_1	0.8544	0.6671	0.2757	1338.07	34.61	7.7406

Scanning Electron Microscopy (SEM)

T SEM analysis was used to visualize the surface morphology and shape of nanoparticles at magnifications ranging from 15,000× to 18,000× in order to capture images. It was found that the Mfx-GNPs have a smooth and spherical surface shown in fig 5.

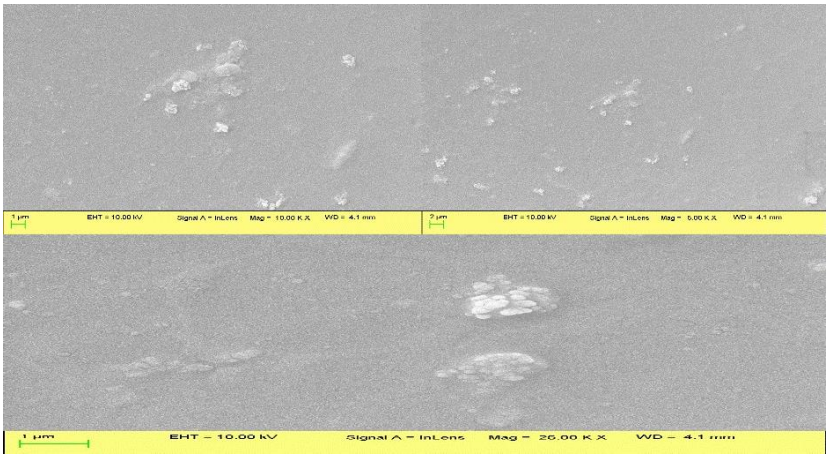

Figure 5: SEM images of the synthesized GNPs using different magnification

Entrapment Efficiency

One important characteristic for characterizing Mfx-GNPs is their loading efficiency. The percentage of Mfx that was effectively loaded or bound to the surface of GNPs was used to measure the loading efficiency of Mfx onto GNPs. Our findings showed a remarkable loading efficiency of around 89%. When the experiment started, 334.4 µg/mL of Mfx was used, and 294.4 µg/mL of the Mfx had firmly bonded to the surface of GNPs.

Mean particle size, polydispersity index (PDI) and zeta potential

The mean particle size, zeta potential and polydispersity index of the developed Mfx-GNPs were determined by (Zetasizer Nano ZS 90, Malvern Instruments, UK). The mean particle size, zeta potential and polydispersity

index of the optimized formulation were found to be 56.25 nm, along with -25.3 (mV) and 0.011 PDI respectively.

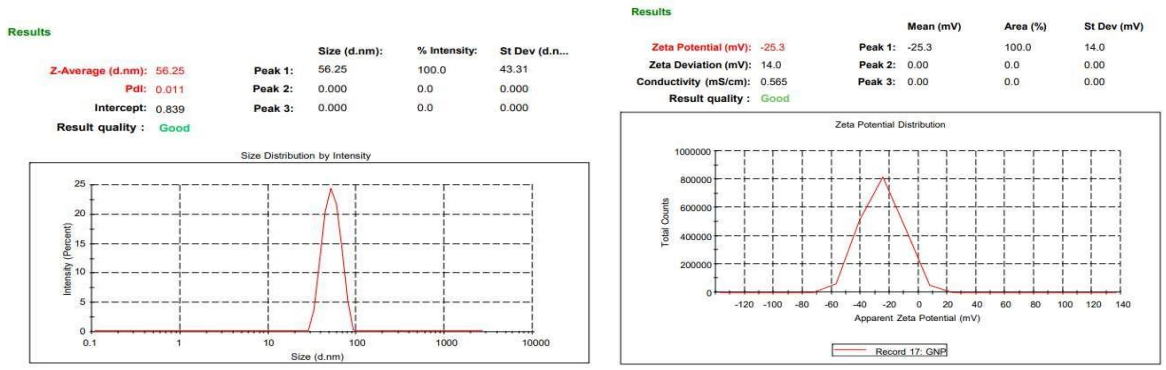

(A) **(B)**

Figure 6: (A) Particle size of Mfx-GNPs (B) Zeta potential of Mfx-GNPs

Fourier Transforms Infrared Spectroscopy (FTIR)

FTIR studies can be adopted to recognize the possible agents/molecules responsible for conjugation and efficient stabilization of the metal nanoparticles. In this study, FTIR spectral analysis was obtained for the confirmation of attachment of Mfx molecules over the surface of GNPs. The major peaks recorded in the pure Mfx sample were attributed to the functional groups: –O–H stretching (3433 cm−1), carboxylic –C=O stretching (1638 cm−1), C–F stretching (1061 cm−1) and C–Cl stretching (771 cm−1), which confirms the purity of the Mfx antibiotic. However, post synthesis of Mfx-GNPs, an elevation in the –O–H stretching peak intensity along with reduction in peak intensities at the respective –C=O stretching, C–F stretching and C–Cl stretching positions were observed, which was attributed to the conformational change occurred in the Mfx after conjugate onto GNPs. Moreover, nitrogen of piperazinyl group of Mfx might have played an important role in the interaction with GNPs. Similar to the present study, other authors also suggested that fluoroquinoloid antibiotics (norfloxacin, ciprofloxacin, and gatifloxacin, moxifloxacin) might interact with GNPs via nitrogen of the piperazinyl group.

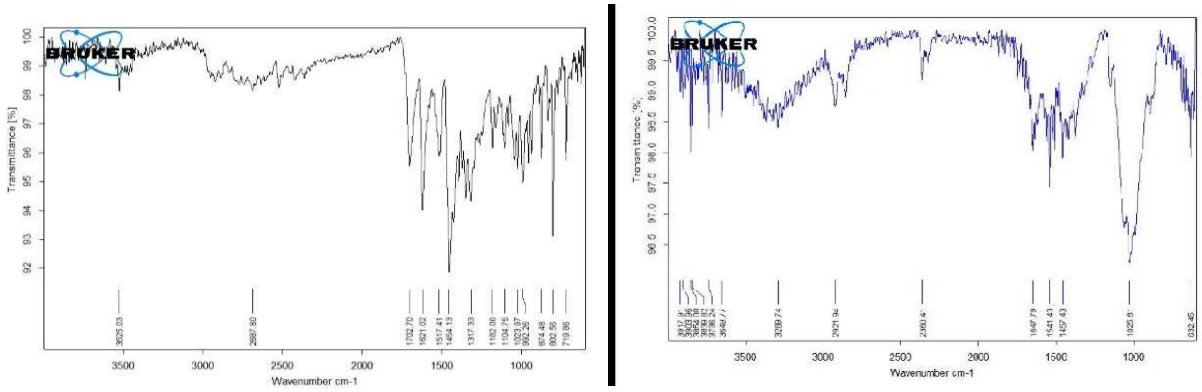

(A) **(B)**

Figure 7: FTIR spectra of (A) Pure Mfx and (B) Mfx-GNPs

The FTIR spectra of a pure drug and a drug plus polymer mixture are displayed in fig 8. The spectral analysis revealed that the peaks of the pure drug and drug polymer mixture did not significantly change. Therefore, there was no specific interaction between the drug and the polymers used in the formulations.

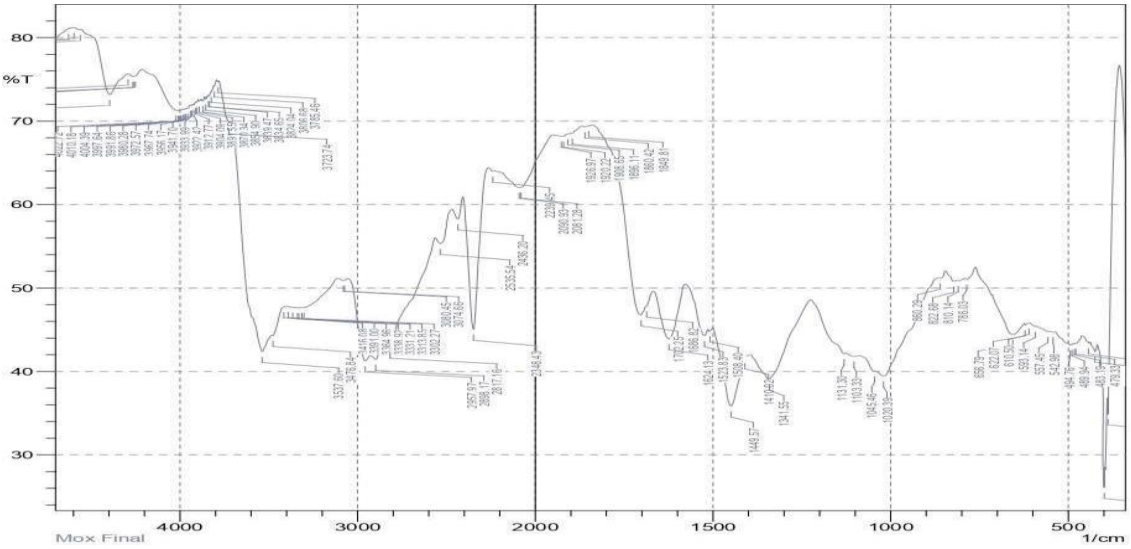

Figure 8: FTIR of final formulation

Differential Scanning Calorimetry

The physical mixture of moxifloxacin Hcl with all excipients and the DSC thermogram of pure moxifloxacin Hcl are compared in Figures 9 and 10. The endothermic peak of moxifloxacin shows long and unique endothermic peak at 261.24 ^{0}C. A distinctive peak at 249.77^{0}C was showed by the physical mixture of the drug and polymers. This result makes it evident that moxifloxacin Hcl and excipients do not interact.

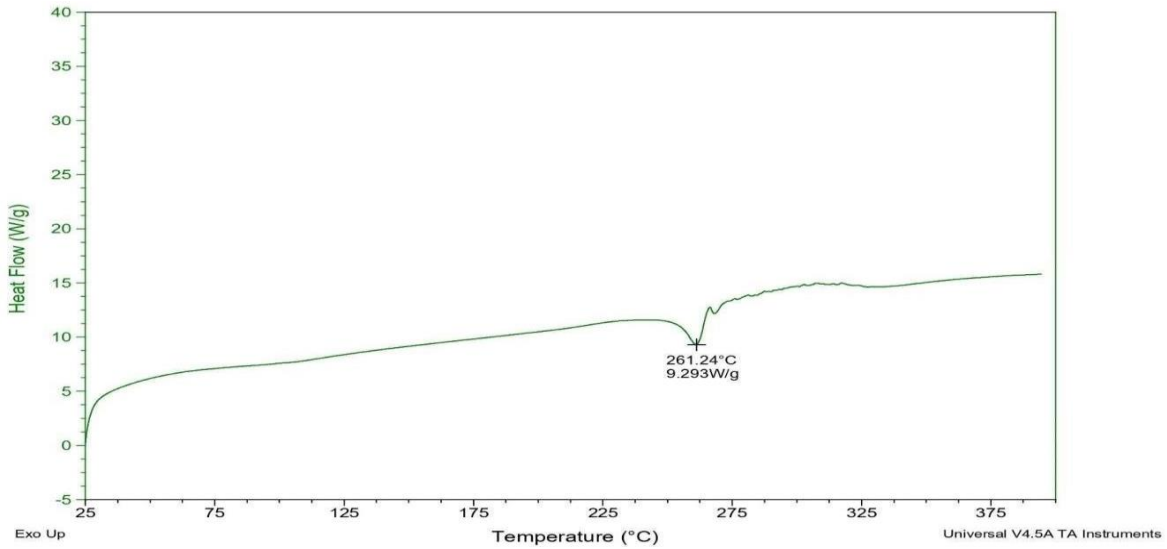

Figure 9: Thermal analysis of Moxifloxacin Hydrochloride

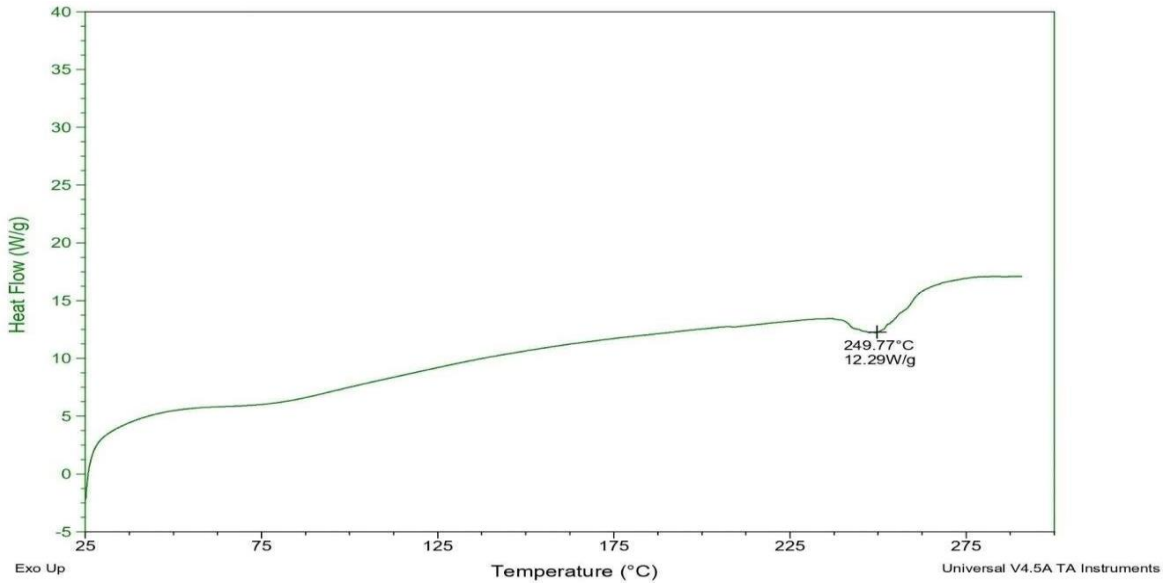

Figure 10: Thermal analysis of Moxifloxacin Hydrochloride + Excipient (Physical mixture)

X-ray Diffraction (XRD) Analysis

X-ray diffraction study was performed to assess the state of loaded drug and to confirm whether it was in microcrystalline form, without polymorph change or transition change in amorphous form. Figure 11 & 12 depicts the diffractograms of the pure drug Moxifloxacin Hydrochloride (Mfx) and Mfx + Excipients. Drug peaks in the formulation was suppressed and this may be attributed to solubility of Mfx in the polymer solution and higher polymer concentration. The peaks of formulation were similar to polymer peaks, indicating that the Mfx-GNPs was completely mixed with the polymer.

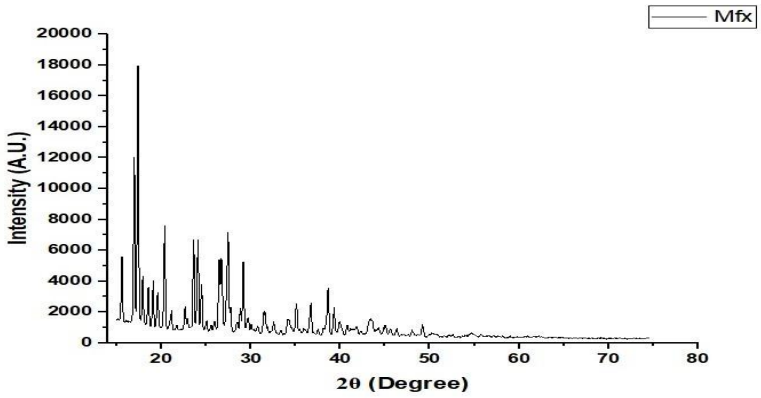

Figure 11: X-ray Diffractogram of Drug-Moxifloxacin Hydrochloride (Mfx)

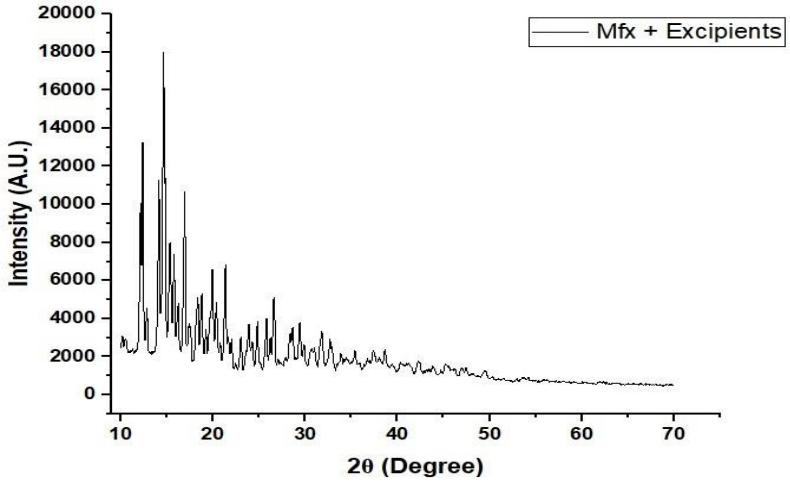

Figure 12: X-ray Diffractogram of Drug-Mfx + Excipients

Clarity

Clarity of all formulations was found satisfactory. The formulations were light yellow in color. Terminal sterilization with autoclaving had no effect on physicochemical properties of the formulation.

Gelling capacity

Within the set of seventeen formulations, some formulation exhibited the best gelling capacity, while some of them showed slow gelation. Table 6 included all of these observations.

Table 7: Gellation Capacity of Mfx-GNPs loaded *In-situ* Gel

S. No.	Formulation	Gelling Capacity
1	F1	+++
2	F2	++
3	F3	++
4	F4	++
5	F5	+++
6	F6	+++
7	F7	++
8	F8	+
9	F9	+++
10	F10	+++
11	F11	++
12	F12	+++
13	F13	+++
14	F14	+++

15	F15	++
16	F16	+++
17	F17	+

- : No Gellation
+ : Slow Gellation and disappear
++ : Gellation fast and remain for some hours
+++ : Gellation immediate and retain for long time

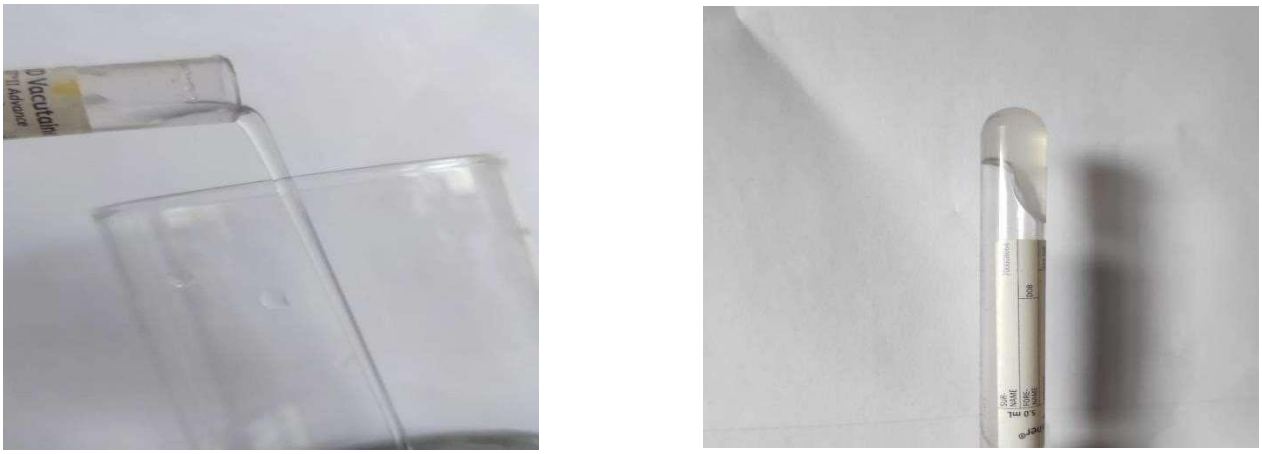

(A) **(B)**

Figure 13: (A) Before Gelling (B) After Gelling

Rheological studies

All of the formulations showed pseudoplastic flow in the eye after gelling and Newtonian flow before to gelling, according to rheological examination. After gelling, there was an increase in viscosity. Furthermore, the gel which is formed in situ need to remain intact for a longer period of time without degrading or dissolving. The results are shown in Table 4.

Measurement of pH

To prevent eye irritation and unpleasantness, the pH of the developed formulation for ophthalmic formulation must be within the normal ocular comfort range (pH 6.6 to 7.8). All developed Mfx-GNPs loaded in-situ gel in this research had mean pH values within the permitted range (6.53 ± 0.03 to 7.86 ± 0.02), therefore minimizing the possibility that instillation into the eye would cause irritation or discomfort.

Sterility Studies

The aforementioned results led to the conclusion that no growth nor turbidity was observed over the 14-day incubation period for any medium. As per Indian Pharmacopoeia 2007 vol. 1, it confirms that the sterilizing procedure was carried out accurately and that optimized in situ gelling systems passed the sterility test. The medium being used is appropriate, as shown by the successful test control. With no turbidity and no microbial growth.

Drug content

Drug content of the prepared Mfx-GNPs loaded in-situ gel was in the range of 98-99% w/w, excluding any possibility for segregation of drug or additives during preparation.

In vitro Drug Release Study

In vitro release studies were done to evaluate the amount of drug released in STF. Periodically samples were withdrawn from the modified dissolution apparatus and analyzed by UV spectrophotometer at 288 nm. The percentage cumulative release of drug was shown in Fig.14

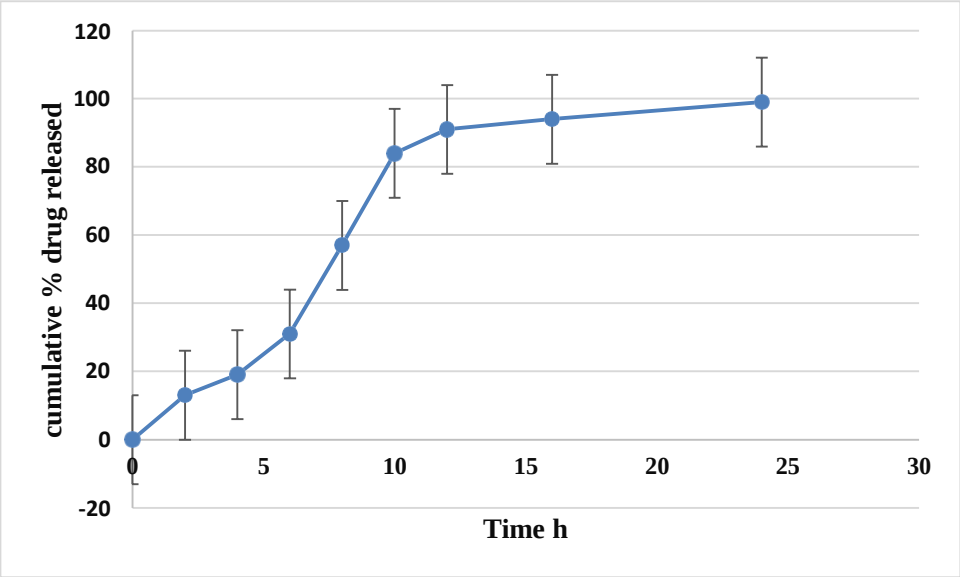

Figure 14: Cumulative % drug release profile graph of the optimized Mfx-GNPs loaded In-Situ gel formulation.

Anti-Bacterial efficacy

Antibacterial efficacy study was performed on Mfx-GNPs loaded in-situ gel using Pseudomonas aeruginosa (ATCC27853) Escherichia coli (ATCC25922), Staphylococcus aureus (ATCC25923), Candida albicans (ATCC14053) and Klebsiella pneumoniae (ATCC700603). The zone of inhibition of Mfx-GNPs loaded in-situ gel formulation found to be 68.34 ± 0.11, 60.75 ± 0.26, 59.61 ± 0.06, 51.58 ± 0.20 and 58.52 ± 0.34 mm, respectively, for bacterial strains. The results of antimicrobial activity are as shown in the Table: 8 and Fig. 15. The study indicated Mfx-GNPs retained its antimicrobial activity when formulated as gel forming ophthalmic system against bacterial strains.

Table 8: Zone of Inhibition

S. No.	Microorganism	Concentration (µg/ml)	Zone of inhibition (mm)	
			Standard (pure drug)	Final formulation
1.	Pseudomonas aeruginosa (ATCC27853)	2µg/ml	65.30 ± 0.16	68.34 ± 0.11

2.	Staphylococcus aureus (ATCC25923)	2µg/ml	46.48 ± 0.33	60.75 ± 0.26
3.	Escherichia coli (ATCC25922)	2µg/ml	52.36 ± 0.26	59.61 ± 0.06
4.	Candida albicans (ATCC14053)	2µg/ml	56.76 ± 0.10	51.58 ± 0.20
5.	Klebsiella pneumoniae (ATCC700603)	2µg/ml	52.57 ± 0.10	58.52 ± 0.34

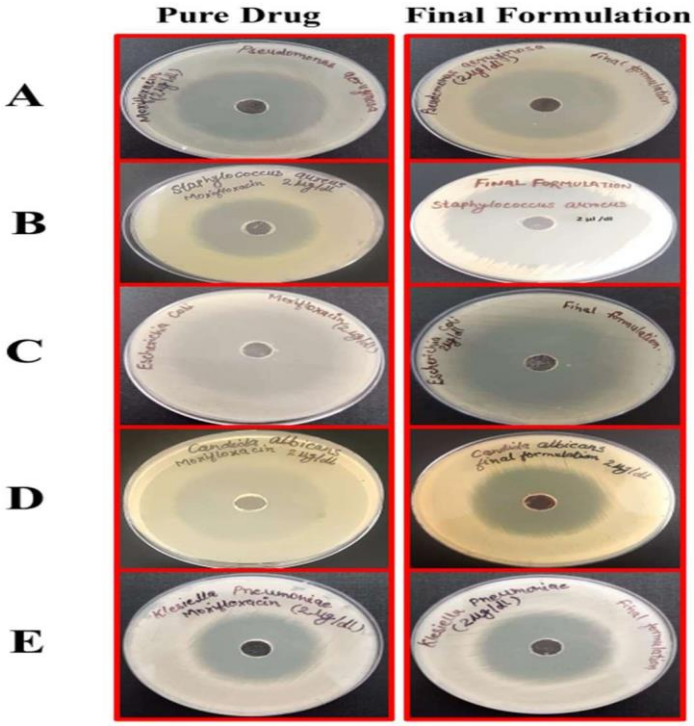

Figure 15: (A) Pseudomonas aeruginosa (B) Staphylococcus aureus (C) Escherichia coli (D) Candida albicans (E) Klebsiella pneumoniae

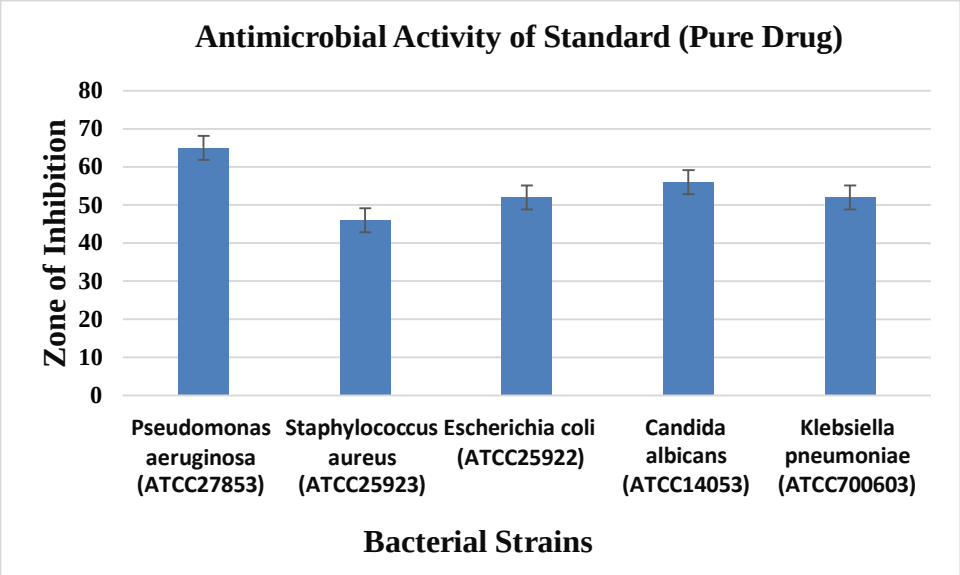

Figure 16: Antimicrobial Activity of Standard (Pure Drug)

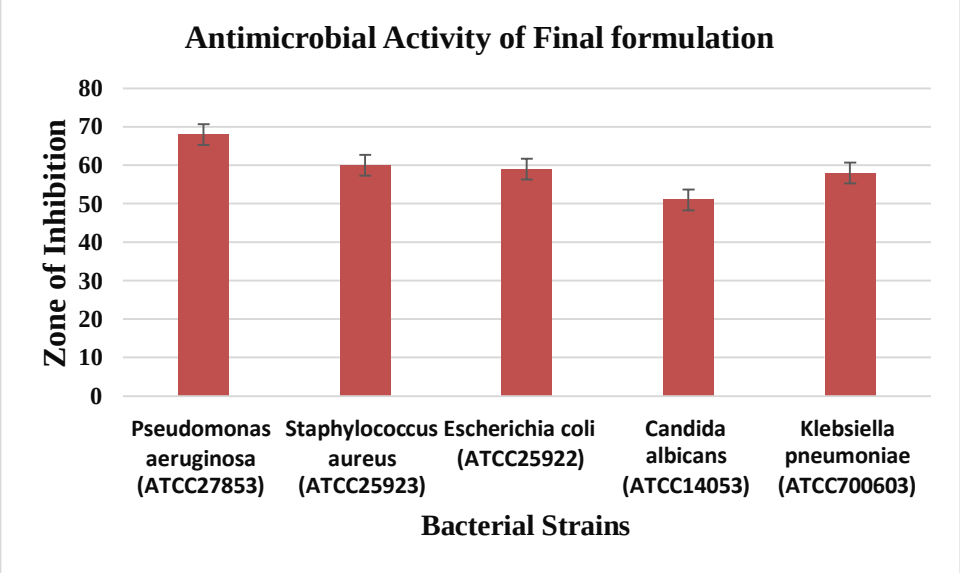

Figure 17: Antimicrobial Activity of Final formulation

Anti-Biofim Activity

The biofilms disrupting the ability of gold nanoparticles were evaluated by light microscopy stained with crystal violet (CV). In control (untreated samples), a mature concrete biofilm is noticed via staining with CV (Fig.18). The staining with CV provides quite important data for good measure of bacterial biofilm mass and does not provide any qualitative insights. As suggested, treated samples with CV showed disorganized bacterial colonies upon increasing concentration of Mfx-GNPs (Fig.18). In our case, a CV dye was used as a bacterial biofilm indicator to stain cells as well as nucleic acids. We acknowledged the dose-dependent reduction of CV, inferring the eradication of biofilm (Fig.18). However, the mechanism of annihilating the bacterial biofilms by Mfx-GNPs is not known. We presume that Mfx-GNPs tend to interact with thick peptidoglycan layer interspersed

by teichoic acids. As a result, accretions of gold nanoparticles occur in bacterial cell membranes leading to lysis of bacterial cells.

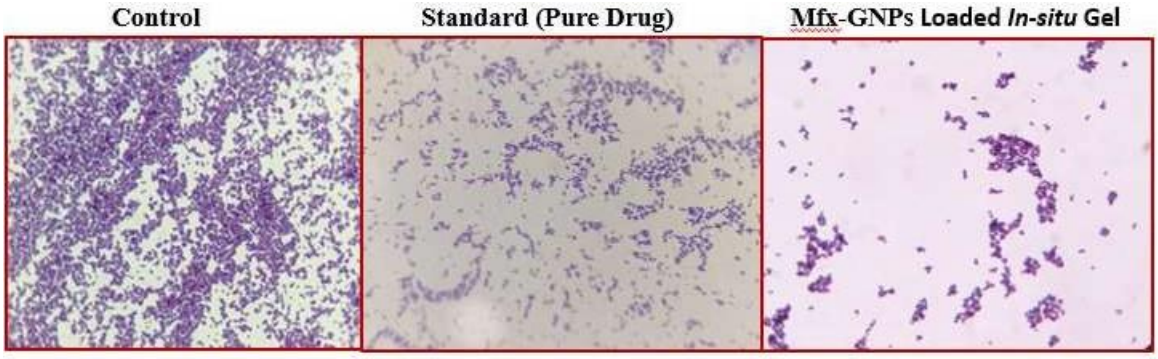

Figure 18: Anti-Biofilm Activity of Pure Drug and Mfx-GNPs Loaded *In-Situ* Gel

Accelerated stability study

The stability data at the end of the 45 days revealed that formulations was found to be stable and efficacious. No change in pH, drug content, gelling capacity, clarity, and appearance were observed.

CONCLUSION:

Despite the challenges in ocular drug delivery, over the past few years, many innovative approaches are being developed to overcome the problems associated with conventional of ophthalmic preparations. The in-situ gelling system is one the promising and extensively studied strategies that could prolong precorneal resident time and offer the sustained release drug delivery, thus improve ocular bioavailability and therapeutic efficacy and reduce systemic absorption and toxicity. The present study demonstrates the formulation of Mfx-GNPs loaded *in-situ* gel. This gold nanoparticles displayed superior antibacterial activity against various bacterial strains and can annihilate the bacterial biofilms. Moxifloxacin hydrochloride, a broad spectrum antibacterial agent used in the treatment of ocular infections, was successfully formulated as in situ gel-forming eye drops. Thus, the developed formulation is a viable alternative to conventional eye drops by virtue of its ability to enhance bioavailability through its longer precorneal residence time and ability to sustain drug release.

Conflicts of interest

The authors confirm that this article has no conflict of interest.

Acknowledgements

The authors are thankful to the Director, University Institute of Pharmacy, and Pt. Sunderlal Sharma Central library, Pt. Ravishankar Shukla University, Raipur, India for providing necessary infrastructure facilities and Inflibnet e-resources.

REFERENCES:

1. Makwana SB, Patel VA, Parmar SJ. Development and characterization of in-situ gel for ophthalmic formulation containing ciprofloxacin hydrochloride. Results in pharma sciences. 2016 Jan 1; 6:1-6. 10.1016/j.rinphs.2015.06.001.

2. Baranowski, P., Karolewicz, B., Gajda, M. and Pluta, J., 2014. Ophthalmic drug dosage forms:

characterisation and research methods. *The Scientific World Journal*, *2014*. 10.1155/2014/861904.

3. Akhter, M.H., Ahmad, I., Alshahrani, M.Y., Al-Harbi, A.I., Khalilullah, H., Afzal, O., Altamimi, A.S., Najib Ullah, S.N.M., Ojha, A. and Karim, S., 2022. Drug delivery challenges and current progress in nanocarrier-based ocular therapeutic system. *Gels*, *8*(2), p.82. org/10.3390/gels8020082.

4. Vigani, B., Rossi, S., Sandri, G., Bonferoni, M.C., Caramella, C.M. and Ferrari, F., 2020. Recent advances in the development of in situ gelling drug delivery systems for non-parenteral administration routes. *Pharmaceutics*, *12*(9), p.859. 10.3390/pharmaceutics12090859.

5. Mandal, S., Thimmasetty, M.K., Prabhushankar, G.L. and Geetha, M.S., 2012. Formulation and evaluation of an in situ gel-forming ophthalmic formulation of moxifloxacin hydrochloride. *International journal of pharmaceutical investigation*, *2*(2), p.78. 10.4103/2230-973X.100042.

6. Liu, Y., Liu, J., Zhang, X., Zhang, R., Huang, Y. and Wu, C., 2010. In situ gelling gelrite/alginate formulations as vehicles for ophthalmic drug delivery. *Aaps PharmSciTech*, *11*, pp.610-620. 10.1208/s12249-010-9413-0.

7. Narayana, S. and Ahmed, M.G., 2022. Design and evaluation of ocular hydrogel containing combination of ofloxacin and dexamethasone for the treatment of conjunctivitis. *Brazilian Journal of Pharmaceutical Sciences*, *58*. org/10.1590/s2175-97902022e20180.

8. Zhao, A., Sun, J. and Liu, Y., 2023. Understanding bacterial biofilms: From definition to treatment strategies. *Frontiers in Cellular and Infection Microbiology*, *13*, p.1137947. org/10.3389/fcimb.2023.1137947.

9. Joshi, A.S., Singh, P. and Mijakovic, I., 2020. Interactions of gold and silver nanoparticles with bacterial biofilms: Molecular interactions behind inhibition and resistance. *International Journal of Molecular Sciences*, *21*(20), p.7658. 10.3390/ijms21207658.

10. Shkodenko, L., Kassirov, I. and Koshel, E., 2020. Metal oxide nanoparticles against bacterial biofilms: Perspectives and limitations. *Microorganisms*, *8*(10), p.1545. org/10.3390/microorganisms8101545.

11. Wang, L., Hu, C. and Shao, L., 2017. The antimicrobial activity of nanoparticles: present situation and prospects for the future. *International journal of nanomedicine*, pp.1227-1249. org/10.2147/IJN.S121956.

12. Nair, A.B., Shah, J., Jacob, S., Al-Dhubiab, B.E., Sreeharsha, N., Morsy, M.A., Gupta, S., Attimarad, M., Shinu, P. and Venugopala, K.N., 2021. Experimental design, formulation and in vivo evaluation of a novel topical in situ gel system to treat ocular infections. *PloS one*, *16*(3), p.e0248857. 10.1371/journal.pone.0248857.

- 13. Srividya, B.J.R.M., Cardoza, R.M. and Amin, P.D., 2001. Sustained ophthalmic delivery of ofloxacin from a pH triggered in situ gelling system. *Journal of controlled release*, *73*(2-3), pp.205-211. 10.1016/s0168-3659(01)00279-6.

14. Tarantino, S., Caricato, A.P., Rinaldi, R., Capomolla, C. and De Matteis, V., 2023. Cancer Treatment Using Different Shapes of Gold-Based Nanomaterials in Combination with Conventional Physical Techniques. *Pharmaceutics*, *15*(2), p.500. org/10.3390/pharmaceutics15020500.

15. Gu, X., Xu, Z., Gu, L., Xu, H., Han, F., Chen, B. and Pan, X., 2021. Preparation and antibacterial properties of gold nanoparticles: A review. *Environmental Chemistry Letters*, *19*, pp.167-187. 10.3390/molecules26195823.

16. Rabiee, N., Ahmadi, S., Akhavan, O. and Luque, R., 2022. Silver and gold nanoparticles for antimicrobial purposes against multi-drug resistance bacteria. *Materials*, *15*(5), p.1799. 10.3390/ma15051799.

17. Yang, Y., Matsubara, S., Nogami, M. and Shi, J., 2007. Controlling the aggregation behavior of gold nanoparticles. *Materials Science and Engineering: B*, *140*(3), pp.172-176. org/10.1016/j.mseb.2007.03.021.

18. Su, C., Huang, K., Li, H.H., Lu, Y.G. and Zheng, D.L., 2020. Antibacterial properties of functionalized gold nanoparticles and their application in oral biology. *Journal of Nanomaterials*, *2020*, pp.1-13. org/10.1155/2020/5616379.

19. Zhao, X., Tang, H. and Jiang, X., 2022. Deploying gold nanomaterials in combating multi-drug-resistant bacteria. *ACS nano*, *16*(7), pp.10066-10087. 10.1021/acsnano.2c02269.

20. Das, P., Ghosh, S. and Nayak, B., 2021. Phyto-fabricated nanoparticles and their anti-biofilm activity: Progress and current status. *Frontiers in Nanotechnology*, *3*, p.739286. org/10.3389/fnano.2021.739286.

21. Koirala S, Nepal P, Ghimire G, Basnet R, Rawat I, Dahal A, Pandey J, Parajuli-Baral K. Formulation and evaluation of mucoadhesive buccal tablets of aceclofenac. Heliyon. 2021 Mar 1; 7(3). 10.1016/j.heliyon.2021.e06439.

22. Dong J, Carpinone PL, Pyrgiotakis G, Demokritou P, Moudgil BM. Synthesis of precision gold nanoparticles using Turkevich method. KONA Powder and Particle Journal. 2020 Jan 10; 37:224-32. 10.14356/kona.2020011.

23. Nisar M, Khan SA, Shah MR, Khan A, Farooq U, Uddin G, Ahmad B. Moxifloxacin-capped noble metal nanoparticles as potential urease inhibitors. New Journal of Chemistry. 2015; 39(10):8080-6. 10.1039/c0xx00000x.

24. Zafar A, Alsaidan OA, Imam SS, Yasir M, Alharbi KS, Khalid M. Formulation and evaluation of moxifloxacin loaded bilosomes in-situ gel: optimization to antibacterial evaluation. Gels. 2022 Jul 4; 8 (7):418. 10.3390/gels8070418.

25. Nair AB, Shah J, Jacob S, Al-Dhubiab BE, Sreeharsha N, Morsy MA, Gupta S, Attimarad M, Shinu P, Venugopala KN. Experimental design, formulation and in vivo evaluation of a novel topical in situ gel system

to treat ocular infections. PloS one. 2021 Mar 19; 16 (3):e0248857. 10.1371/journal.pone.0248857.

26. Zhu S, Hong M, Liu C, Pei Y. Application of Box-Behnken design in understanding the quality of genistein self-nanoemulsified drug delivery systems and optimizing its formulation. Pharmaceutical development and technology. 2009 Dec 1; 14(6):642-9. 10.3109/10837450902882385.

27. Yadav P, Rastogi V, Verma A. Application of Box–Behnken design and desirability function in the development and optimization of self-nanoemulsifying drug delivery system for enhanced dissolution of ezetimibe. Future Journal of Pharmaceutical Sciences. 2020 Dec; 6 (1):1-20. org/10.1186/s43094-020-00023-3.

28. Kalbhare SB, Redasani VK, Bhandwalkar MJ, Pawar RK, Bhagwat AM. Role of aminated derivatives of natural gum in release modulating matrix systems of losartan potassium: Optimization of formulation using Box-Behnken design. Asian Journal of Pharmaceutical Research. 2021; 11 (2):73-84. 10.5958/2231–5691.

29. Lv Y, He H, Qi J, Lu Y, Zhao W, Dong X, Wu W. Visual validation of the measurement of entrapment efficiency of drug nanocarriers. International journal of pharmaceutics. 2018 Aug 25; 547 (1-2):395-403. 10.1016/j.ijpharm.2018.06.025.

30. Hussain MH, Abu Bakar NF, Mustapa AN, Low KF, Othman NH, Adam F. Synthesis of various size gold nanoparticles by chemical reduction method with different solvent polarity. Nanoscale research letters. 2020 Dec; 15: 1-10. org/10.1186/s11671-020-03370-5.

31. Karimi S, Moshaii A, Nikkhah M. Controlled synthesis of colloidal monodisperse gold nanoparticles in a wide range of sizes; investigating the effect of reducing agent. Materials Research Express. 2019 Nov 1; 6 (11):1150f2. 10.1088/2053-1591/ab3e13.

32. Dzimitrowicz A, Jamroz P, Sergiel I, Kozlecki T, Pohl P. Preparation and characterization of gold nanoparticles prepared with aqueous extracts of Lamiaceae plants and the effect of follow-up treatment with atmospheric pressure glow microdischarge. Arabian Journal of Chemistry. 2019 Dec 1; 12(8):4118-30. org/10.1016/j.arabjc.2016.04.004.

33. Chadha, R. and Bhandari, S., 2014. Drug–excipient compatibility screening—role of thermoanalytical and spectroscopic techniques. *Journal of pharmaceutical and biomedical analysis*, *87*, pp.82-97. 10.1016/j.jpba.2013.06.016.

34. Asnag GM, Oraby AH, Abdelghany AM. Green synthesis of gold nanoparticles and its effect on the optical, thermal and electrical properties of carboxymethyl cellulose. Composites Part B: Engineering. 2019 Sep 1; 172: 436-46. org/10.1016/j.compositesb.2019.05.044.

35. Kalaria VJ, Saisivam S, Alshishani A, Aljariri Alhesan JS, Chakraborty S, Rahamathulla M. Design and evaluation of in situ gel eye drops containing nanoparticles of Gemifloxacin Mesylate. Drug Delivery. 2023

Dec 31; 30(1):2185180. org/10.1080/10717544.2023.2185180

36. Endla P, Radhika V. Fabrication and evaluation of gold nanoparticles by ball milling, Hall-Williamson and x-ray diffraction method. Materials Today: Proceedings. 2021 Jan 1; 47: 4993-5. org/10.1016/j.matpr.2021.04.451

37. Srividya, B.J.R.M., Cardoza, R.M. and Amin, P.D., 2001. Sustained ophthalmic delivery of ofloxacin from a pH triggered in situ gelling system. *Journal of controlled release*, *73*(2-3), pp.205-211. 10.1016/s0168-3659(01)00279-6.

38. Nayak, N.S., Bharani, S.S. and Thakur, R.S., 2012. Formulation and evaluation of pH triggered in situ ophthalmic gel of Moxifloxacin hydrochloride. *Int J Pharm PharmSci*, *4*(2), pp.452-459.

39. Liu, Y., Liu, J., Zhang, X., Zhang, R., Huang, Y. and Wu, C., 2010. In situ gelling gelrite/alginate formulations as vehicles for ophthalmic drug delivery. *Aaps PharmSciTech*, *11*, pp.610-620. 10.1208/s12249-010-9413-0.

40. Narayana, S. and Ahmed, M.G., 2022. Design and evaluation of ocular hydrogel containing combination of ofloxacin and dexamethasone for the treatment of conjunctivitis. *Brazilian Journal of Pharmaceutical Sciences*, *58*. org/10.1590/s2175-97902022e20180.

41. Garala K, Joshi P, Shah M, Ramkishan A, Patel J. Formulation and evaluation of periodontal in situ gel. International journal of pharmaceutical investigation. 2013 Jan; 3(1):29. 10.4103/2230-973X.108961.

42. Sriamornsak P, Nunthanid J, Cheewatanakornkool K, Manchun S. Effect of drug loading method on drug content and drug release from calcium pectinate gel beads. AAPS PharmSciTech. 2010 Sep; 11:1315-9. 10.1208/s12249-010-9513-x.

43. Mandal S, Thimmasetty MK, Prabhushankar GL, Geetha MS. Formulation and evaluation of an in situ gel-forming ophthalmic formulation of moxifloxacin hydrochloride. International journal of pharmaceutical investigation. 2012 Apr; 2(2):78. 10.4103/2230-973X.100042.

44. Bao L, Peng R, Ren X, Ma R, Li J, Wang Y. Analysis of some common pathogens and their drug resistance to antibiotics. Pakistan journal of medical sciences. 2013 Jan; 29(1):135. 10.12669/pjms.291.2744.

45. Berini F, Orlandi VT, Gamberoni F, Martegani E, Armenia I, Gornati R, Bernardini G, Marinelli F. Antimicrobial activity of nanoconjugated glycopeptide antibiotics and their effect on Staphylococcus aureus biofilm. Frontiers in Microbiology. 2021 Dec 2; 12: 657431. 10.3389/fmicb.2021.657431.